

Two dimensional graphene derivatives supported isolated gold nanoparticles as an efficient SERS substrate

Shiju Abraham^{a,b}, Matthias König^b, Shobhit Pandey^c, Sunil K Srivastava^d,
Bernd Walkenfort^b and Anchal Srivastava^a

^aDepartment of Physics, Banaras Hindu University, Varanasi-221 005, India

^bFaculty of Chemistry, University of Duisburg, 45141 Essen, Germany

^cMetallurgical Engineering Department, Indian Institute of Technology – (BHU), Varanasi-221 005

^dDepartment of Pure and Applied Physics, Guru Ghasidas University, Bilaspur- 495 009, India

(Dedicated to Professor Wolfgang Kiefer on the occasion of his 75th birthday)

The present work accomplishes surface enhanced Raman scattering (SERS) studies using the combination of stable, diluted and isolated gold nanoparticles (Au NPs) of tailored size (~ 50 nm) and distribution on two dimensional carbon nanostructures (2D-CNS) i.e. graphene oxide (GO) and reduced graphene oxide (RGO). Fabricated using a simple, quick and cost effective method, these SERS substrates have enough synergistic enhancement from each Au NPs and underlying CNS matrix with sensitivity enough to easily detect 10^{-6} molar concentrations of analyte, 4-mercaptobenzoic acid (4-MBA). Further, uniform distribution of Au NPs ensures great reproducibility showing potential for standardization in future. © Anita Publications. All rights reserved.

Keywords: Surface enhanced Raman scattering (SERS), Nanoparticles, Graphene oxide (GO), 4-mercaptobenzoic acid (4-MBA)

1 Introduction

Surface-enhanced Raman scattering (SERS) is a surface selective and highly sensitive spectroscopic technique for molecular detection and surface analysis [1,2]. SERS offers higher magnitude of increased intensity and suppresses the fluorescence signal while selectively enhancing the Raman signal, and produces chemical fingerprinting with sensitivity enough to enable single-molecule detection [3]. Two widely accepted enhancement mechanisms are the dominant electromagnetic mechanism (EM) (contributing about 10⁸ of enhancement) and the chemical mechanism (CM) (contributing one or two orders of enhancement), together contributing the overall enhancement [4]. The long range nature of EM relies on the roughness, high curves or gapped metal regions of the substrate in order to develop localized electromagnetic field regions called as “hot” spots. In this respect, rough noble metal nanoparticles substrates, especially Au NPs having good curvature and required optical properties for enhanced surface plasmons on excitation, proved out to be one of the most popular traditional SERS substrates with additional advantages such as biocompatibility, stability, controllable size and shape distributions [5,6]. Mostly, due to complex distribution of molecules on SERS substrate, molecules near the hot spots keep on fluctuating, which is further aggravated by other factors like chemical interactions between the molecules and the metal substrate, chemical adsorption-induced vibrations, molecular deformation and distortion, etc. [7,8]. These disadvantages demand new materials for SERS substrates, which can be fabricated uniformly and economically with particles size small enough that an isolated particle can give the required localized surface plasmon resonance effect.

Corresponding author :

e-mail: anchalbhu@gmail.com, phone: +91 9453203122 (Anchal Srivastava)

Often termed as a “first layer effect”; unlike EM, CM is a short range effect which requires the distance between the molecule and the substrate to be below 0.2 nm. Further, the charge transfer between molecule and substrate is possible by having the Fermi level of the metal substrate symmetrically aligned with the highest occupied molecular orbital (HOMO) and lowest unoccupied molecular orbital (LUMO) of the molecule [1,9]. These requirements mark the inefficiency of CM in case of noble nanoparticles based SERS substrates, but paved the way for graphene substrates based SERS; called now as Graphene Enhanced Raman Spectroscopy (GERS). In case of graphene, relatively smooth surface, visible range optical transitions [10], and lower surface plasmon [11] make EM ineffective, making CM as the dominant mechanism. However, unlike metal substrates, the Raman enhancements are limited and not enough for standardization [12]. Nevertheless, flexibility offered by graphene and its derivatives and particularly their ability to combine with metal nanoparticles attests its potential as a promising matrix for forming hybrids [13] which can take advantage of both EM and synergistically enhanced CM, for an overall commendable Raman enhancement; the prime motivation of the present work.

With this aim, the present work utilizes Au NPs supported 2D-CNS matrix, as a commendable SERS substrate for testing the efficacy of the Raman Marker; 4-MBA. Finally, in order to produce reproducibility enabling future standardization, the present work uses the enhancement upraised from isolated Au NPs of tailored size decorated at distances higher than the spectral resolution of the exciting source, still producing commendable enhancements without any signal degradation; enough for detecting smallest of the concentrations (10^{-6} M) of the Raman marker.

2 Experimental

Typically the 2D- CNS used here (GO and RGO) were produced using the earlier reports [14,15] (supplementary information). Further to produce non agglomerating Au NPs with tailored size, seeded-growth method proposed by Perrault *et al* was followed [16] (Supplementary information). However, in order to maximize the localized surface plasmon resonance (LSPR) effect for maximum enhancement from each Au NPs, the size was then tailored to 50 nm while simultaneously stabilizing with, polyvinylpyrrolidone (PVP).

The 2D- CNS- Au nanoparticles composites were prepared by simply adding 300 μ L of diluted spherical Au NPs into 700 μ l of 2 mg/ mL (in distilled water) dispersion of 2D- CNS, succeeded by sonication and storage in vibration stand until thin film formation (supplementary information). These two composites i.e RGO- Au NP and GO- Au NP were then uniformly spin coated covering entire (5 \times 5) mm² silicon substrate to form the SERS substrate on which 5 μ L of Raman marker solution of 4-MBA (1 μ M) was then incubated for overnight at room temperature.

3 Results and Discussion

The transmission electron microscopy (TEM) image shown in Fig 1 manifests the homogenously stabilized Au NPs, which were well separated and spherical in shape (~50 nm). Figure 2(a) shows the TEM image of GO sheets, which is non-contaminated, continuous and few layered in nature. Figure 2 (b) corresponding to TEM of GO-Au NPs, clearly shows a single Au NP is decorated on $\sim(2 \times 2)$ μ m² area. The Au NPs have required shape (spherical) and size (50 nm) for effective Raman enhancement effect, while the distribution is such that, the distance between Au NPs exceeds the spectral resolution of the laser, enabling isolated particles enhancement. Figure 2(c) shows the TEM image of few layered RGO sheets of long lateral uniformity like GO. Similarly RGO-Au NPs shown in Fig 2(d) denotes the isolated Au NP distribution on the RGO surfaces as in case of GO.

In order to check the reproducibility and potential to be used as a standardized SERS substrate in future, the work involves Raman mapping (using confocal Raman microscope of WITec Alpha 300R, 632.8

nm laser line) of $(100 \times 100) \mu\text{m}^2$ area on substrate scanned with an interval of $2 \mu\text{m}$ with an integration time of 1s. Figure 3 represents a simplified schematic of the SERS substrate and the SERS signal enhancement obtained.

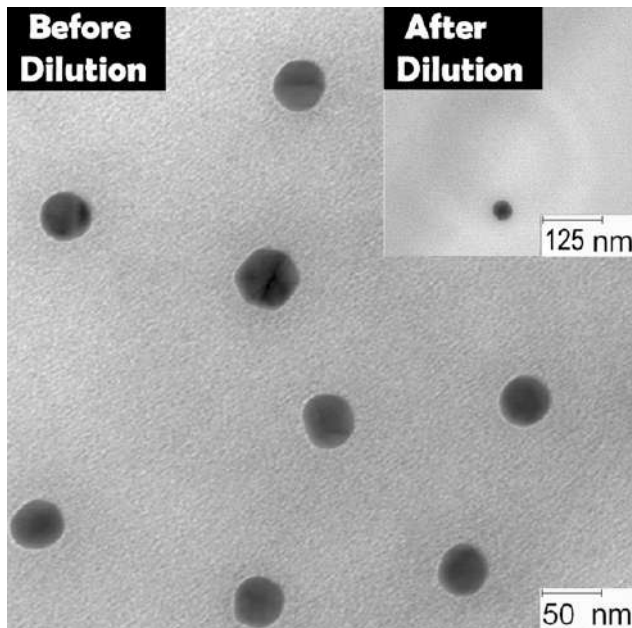


Fig 1. TEM Image of Au NPs; on inset, isolated Au N

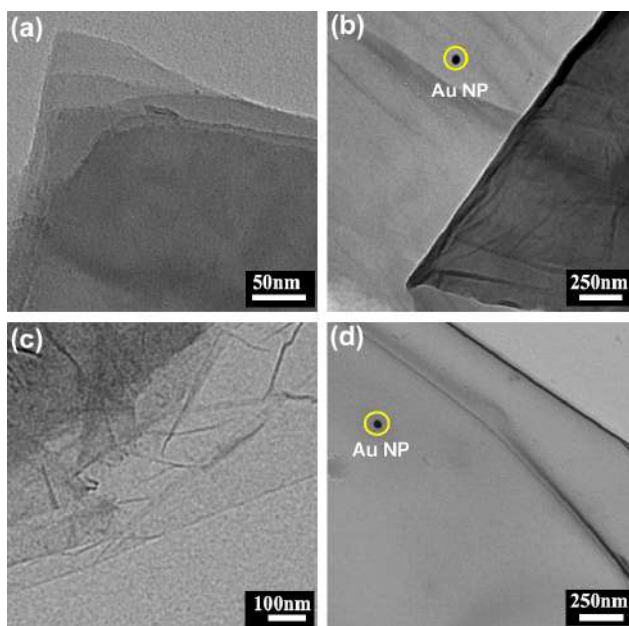


Fig 2. TEM Images of (a) Few layered GO, (b) GO-Au NPs (c) Few layered RGO, (d) RGO-Au NPs

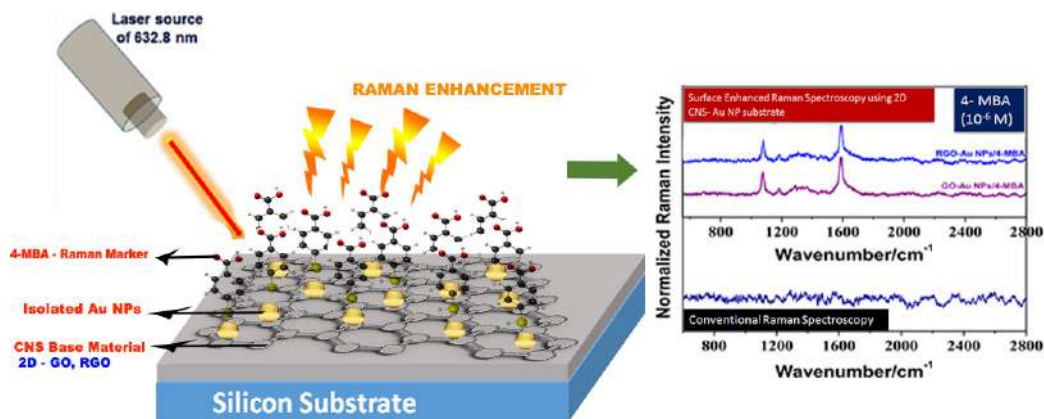


Fig 3. Schematic illustrating the SERS substrate and the Raman enhancement obtained

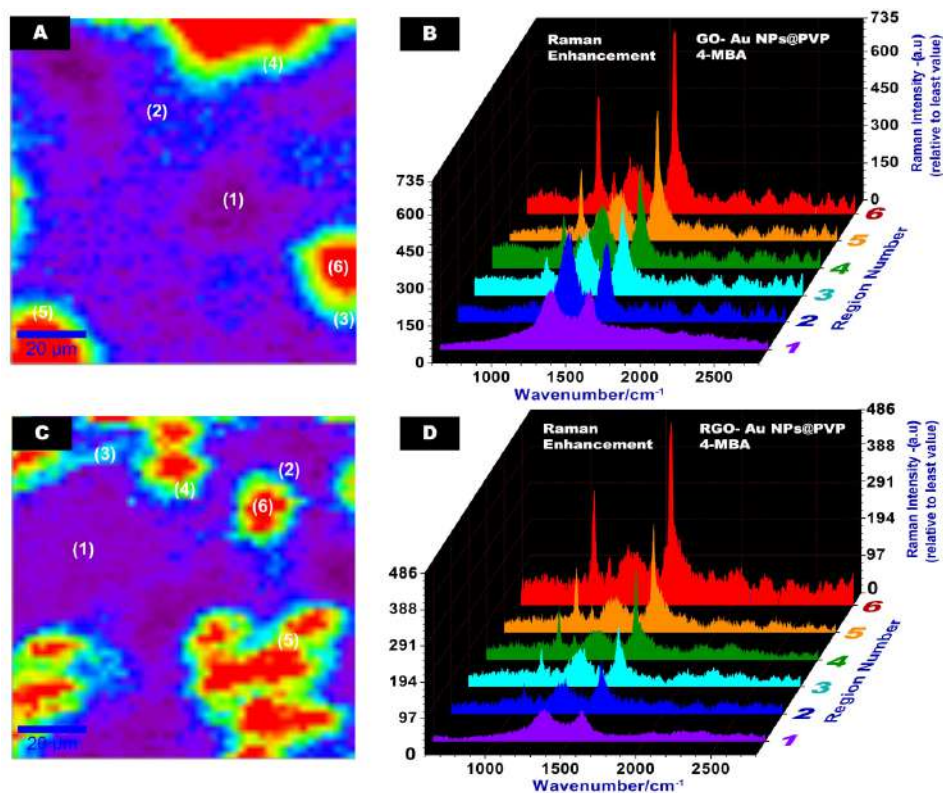


Fig 4. (a) Raman mapping image of GO-Au NPs-4-MBA; (b) Corresponding six point's 3D-SERS spectra. (c) The Raman mapping image RGO-Au NPs-4-MBA, (d) 3D- SERS spectra of RGO-Au NPs-4-MBA.

Raman imaging of GO-Au NPs- 4-MBA defined for the peak centered at 1585 cm^{-1} through the intensity color profile is shown in Fig 4 (a). The well-defined colored region is a profile for the prominent 4-MBA band centered $\sim 1585\text{ cm}^{-1}$ ($\nu(\text{CC})$ ring stretching). In the color profile, the intensity increases from violet to red. Evidently, the center part of the substrate is more or less occupied with violet and blue color, indicating its more GO nature rather than GO-Au NPs. So the maximum intensity (red color) region

indicates the maximum probable place where Au NPs were decorated and are bonded towards 4-MBA. These findings can be confirmed by the corresponding Raman spectrum of the six different regions (violet to red) (Fig 4 (b)). From the cyan to red color (marked 3 to 6), the corresponding Raman spectrum gives well defined peaks of the Raman marker 4-MBA at 1585, 1175, 1070 and 1340 cm^{-1} even for the low concentration (1 μM) and amount of Raman reporter molecule, attesting substantial Raman enhancement. Also a low profile D ($\sim 1350 \text{ cm}^{-1}$) and G-Band ($\sim 1580 \text{ cm}^{-1}$) of GO can be observed on the same spectrum. But in region 1 and 2, the D and G-Band are more prominent due to the CNS base material contribution. Figure 4 (c) represents the Raman mapping image of RGO-Au NPs-4-MBA and the 4-MBA field is more nicely distributed here (red region). In the corresponding Raman spectra (Fig 4(d)), a more defined 4-MBA characteristics peak can be observed throughout the region 2 to 5. So, both SERS substrates are observed to be good base materials utilizing both the EM and synergistically enhanced CM, to detect effectively and quickly even the very low concentration of Raman reporter molecule (1 μM), which is impossible to detect using normal RS [17].

4 Conclusions

The present work introduces a simple and quick chemical method to fabricate highly efficient SERS substrates based on Au NPs and 2D-CNS (graphene derivatives) combination. The proposed substrates have commendable Raman enhancement, taking the advantage of both; i.e. EM from the Au NPs and synergistically enhanced CM from Au NP decorated GO/RGO matrix. The tailored Au NPs have a size of 50 nm to ensure maximum enhancement at the used excitation source (632.5 nm). Further, their distribution is such that the distance between the nanoparticles is greater than the spectral resolution of the excitation source. These factors enable enhancement which is enough to detect 10^{-6} M concentrations of analyte with appreciable sensitivity. Further, the uniform distribution and isolated particle dependence for enhancement, cuts down the ambiguity of variations in hot spot regions, thereby powering these substrates with great reproducibility; suggesting great potential for standardization in future.

Acknowledgments

SA and SKSre thankful to Alexander von Humboldt for supporting this research work through AvH Research Group Linkage Program. AS acknowledges CAS program sponsored by UGC at Department of Physics, B. H. U and DST project (No.:DST/TSG/PT/2012/68), New Delhi, India for financial assistance.

References

1. Campion A, Kambhampati P, *Chem Soc Rev*, 27(1998)241-250.
2. Schlücker S, *Angew Chemie Int Ed*, 53(2014)4756-4795.
3. Nie S, Emory S R, *Science*, 275(1997)1102-1106.
4. Lin C -C, Yang Y -M, Chen Y -F, Yang T -S, Chang H -C, *Biosens Bioelectron*, 24 (2008)178-183.
5. Talley C E, Jackson J B, Oubre C, Grady N K, Hollars C W, Lane S M, Huser T R, Nordlander P, Halas N J, *Nano Lett*, 5(2005)1569-1574.
6. Song J, Cheng S, Li H, Guo H, Xu S, Xu W, *Mater Lett*, 135(2014)214-217.
7. Le Ru E, Etchegoin P, *Principles of Surface-Enhanced Raman Spectroscopy: And Related Plasmonic Effects*, (Elsevier), 2008.
8. Li J F, Huang Y F, Ding Y, Yang Z L, Li S B, Zhou X S, Fan F R, Zhang W, Zhou Z Y, Wu D Y, *Nature*, 464 (2010)392-395.
9. Otto A, *J Raman Spectrosc*, 36(2005)497-509.
10. Bruna M, Borini S, *Appl. Phys Lett*, 94(2009)31901; doi.org/10.1063/1.3073717.
11. Rana F, *Nanotechnology, IEEE Trans*, 7(2008)91-99.

12. Ling X, Wu J, Xie L, Zhang J, *J Phys Chem C*, 117(2013)2369-2376.
13. Khorasaninejad M, Raeis-Zadeh S M, Jafarlou S, Wesolowski M J, Daley C R, Flannery J B, Forrest J, Safavi-Naeini S, Saini S S, *Sci. Rep.*, 3(2013) 2936: 1-7; doi:10.1038/srep02936
14. Marcano D C, Kosynkin D V, Berlin J M, Sinitskii A, Sun Z, Slesarev A, Alemany L B, Lu W, Tour J M, *ACS Nano*, 4 (2010)4806-4814.
15. Li D, Müller M B, Gilje S, Kaner R B, Wallace G G, *Nat Nanotechnol*, 3(2008)101-105.
16. Perrault S D, Chan W C W, *J Am Chem Soc*, 131(2009)17042-17043.
17. Hsieh C -W, Lin P -Y, Hsieh S, *J Nanophotonics*, 6 (2012)63501.1-6.

[Received: 30.09.2015; accepted:15.10.2015]